A PK-PD Model of Ketamine-Induced High-Frequency Oscillations.

Francisco J. Flores[1,2,*†], ShiNung Ching[1,2,3,†], Katharine Hartnack[1], Amanda B. Fath[4], Patrick L. Purdon[1,2], Matthew A. Wilson[5], Emery N. Brown[1,2,6,7].

1 Department of Anesthesia, Critical Care, and Pain Medicine, Massachusetts General Hospital and Harvard Medical School, Boston, MA, USA.
2 Department of Brain and Cognitive Sciences, Massachusetts Institute of Technology, Cambridge, MA, USA.
3 Department of Mathematics and Statistics, Boston University, Boston, MA, USA.
4 Wellesley College, Wellesley, MA.
5 Picower Institute for Learning and Memory, Massachusetts Institute of Technology, Cambridge, MA, USA.
6 Harvard-MIT division of Health Sciences and Technology, Cambridge, MA, USA.
7 Institute for Medical Engineering and Science, Massachusetts Institute of Technology, Cambridge, MA, USA.
†Joint first authors. ∗E-mail: fjflores@neurostat.mit.edu

Abstract

Objective. Ketamine is a widely used drug with clinical and research applications, and also known to be used as a recreational drug. Ketamine produces conspicuous changes in the electrocorticographic (ECoG) signals observed both in humans and rodents. In rodents, the intracranial ECoG displays a High-Frequency Oscillation (HFO) which power is modulated non-linearly by ketamine dose. Despite the widespread use of ketamine there is no model description of the relationship between the pharmacokinetic-pharmacodynamics (PK-PD) of ketamine and the observed HFO power. *Approach.* In the present study, we developed a PK-PD model based on estimated ketamine concentration, its known pharmacological actions, and observed ECoG effects. The main pharmacological action of ketamine is antagonism of the NMDA receptor (NMDAR), which in rodents is accompanied by a high-frequency oscillation (HFO) observed in the ECoG. At high doses, however, ketamine also acts at non-NMDAR sites, produces loss of consciousness, and the transient disappearance of the HFO. We propose a two-compartment PK model that represents the concentration of ketamine, and a PD model based in opposing effects of the NMDAR and non-NMDAR actions on the HFO power. *Main results.* We recorded ECoG from the cortex of rats after two doses of ketamine, and extracted the HFO power from the ECoG

spectrograms. We fit the PK-PD model to the time course of the HFO power, and showed that the model reproduces the dose-dependent profile of the HFO power. The model provides good fits even in the presence of high variability in HFO power across animals. As expected, the model does not provide good fits to the HFO power after dosing the pure NMDAR antagonist MK-801. *Significance.* Our study provides a simple model to relate the observed electrophysiological effects of ketamine to its actions at the molecular level at different concentrations. This will improve the study of ketamine and rodent models of schizophrenia to better understand the wide and divergent range of effects that ketamine has.

1 Introduction

Ketamine is an important therapeutic drug. It has antinociceptive actions [1] and is widely used clinically as an analgesic [2], as an anesthetic adjuvant [3], and more recently as an antidepressant in chronic depression treatment [4]. For many years in basic research, ketamine has been the principal pharmacological model to study schizophrenia [5]. In addition, there is a long-standing interest in studying how ketamine alters arousal, cognitive and physiological states because of its popular use as a recreational drug [6]. The main pharmacological action of ketamine is antagonism of the NMDA receptor (NMDAR) [7,8], but it is also known to act at non-NMDAR sites, including: HCN1 receptors, $5HT_2A$ serotonergic receptors, D_2 dopamine receptors, M1-M3 muscarinic receptors, and opiate receptors [9–13]. While most of the physiological effects of ketamine can be attributed to NMDAR antagonism, the actions of ketamine at HCN1 receptors are thought to contribute to its anesthetic properties [9, 14].

In rodents, the administration of low doses of ketamine produces hyperactivity. This behavioral effect manifests itself as rapid locomotion, excessive grooming, and tail chasing [15]. The amount of hyperactivity correlates with the power of local field potential recordings in the 130–160 Hz frequency range, known as High-Frequency Oscillation (HFO) [15,16]. The HFO becomes highly coherent in the basal ganglia motor circuit during ketamine-induced hyperactivity [17]. Therefore, the HFO power seems to be related to the behavioral state of the animal. However, the HFO power is non-linearly modulated by the concentration of ketamine. The HFO power decreases shortly after ketamine dosing in a dose dependent manner [17], and it disappears shortly after an anesthetic dose of ketamine [15]. Given the importance of ketamine in clinical and basic research, a pharmacodynamic (PD) model linking the pharmacokinetics (PK) of ketamine with HFO power will prove helpful to objectively monitor ketamine effects in rodents and humans. However, such PK-PD model does not exist yet.

We developed a PK-PD model to relate the NMDAR and non-NMDAR effects of ke-

tamine to the time course of the HFO power observed in the rodent electrocorticogram (ECoG). Several other NMDAR antagonists also produce the HFO, providing evidence for the direct relationship between HFO and NMDAR antagonism [18–20]. The model is based on the difference interaction between NMDAR and non-NMDAR actions of ketamine; the non-NMDAR actions take precedence at higher ketamine concentrations and account for the non-linear relationship between HFO power and ketamine concentration. We tested the model by fitting it to the time course of the HFO power recorded from the cortex of freely moving rats. We tested the concentration dependence of the HFO power by dosing the animals with a low and a high dose of ketamine. We also ensured that the HFO is due to NMDAR antagonism by recording ECoG after injections of MK-801, a selective NMDAR antagonist. The non-linear dependence of HFO power on ketamine concentration is well described by the proposed difference PK-PD model across multiple animals and ketamine doses.

2 Theory

2.1 PK and PD models:

We assume that ketamine concentration in the brain follows a two-compartment PK model with first-order elimination, similar to models described before for other anesthetics [21–23]. The compartments are an ancillary compartment, $C_a(t)$, and a brain compartment $C_b(t)$. The latest represents the estimated time course of ketamine concentration in the brain. The temporal dynamics of the two compartments are governed by the differential equation:

$$\frac{dC(t)}{dt} = \mathbf{A}C(t) + \mathbf{u}(\mathbf{t}) \tag{1}$$

where $C(t) = [C_a(t), C_b(t)]$ is the state vector and $\mathbf{A}$ is the matrix of rate constants,

$$\mathbf{A} = \begin{bmatrix} -(k_{el} + k_{ab}) & k_{ba} \\ k_{ab} & -k_{ba} \end{bmatrix} \tag{2}$$

where k_{ab} governs the transfer rate from the ancillary compartment to the brain compartment, and k_{ba} governs the transfer rate in the opposite direction. The rate constant k_{el} governs the elimination rate from the ancillary compartment. The input to the compartmental model is denoted $\mathbf{u}$, and corresponds to

$$\mathbf{u}(\mathbf{t}) = \begin{bmatrix} I(t) \\ 0 \end{bmatrix} \tag{3}$$

where $I(t)$ defines the injection of the drug into the system. Because in our study ketamine is administered as a single bolus injection, we model $I(t)$ as a Dirac delta function.

Next, we defined a non-monotonic PD model, that provides the non-linear relationship between PK and the time course of HFO power. To achieve this, first we propose that the HFO power due solely to NMDAR antagonism can be described by an E_{max} monotonic function of the Hill-type [24]:

$$E_{NMDAR} = \frac{E_{max} C_b^N}{EC_{50,+}^N + C_b^N} \tag{4}$$

where E_{NMDAR} is the effect that depends purely on NMDAR actions, E_{max} is the maximum drug effect, N is the Hill coefficient that determines the shape of the concentration-effect curve, and $EC_{50,+}$ is the concentration at half-maximal effect (figure 1B, continuous red line) for the NMDAR actions of ketamine. The subscript + means that NMDAR antagonism has a positive effect on the HFO power. The assumption of a Hill-type curve is supported by *in vitro* studies, where it has been shown that binding of ketamine and MK-801 to the NMDAR follows a curve of the Hill-type [10].

The HFO power decreases during loss of righting reflex produced by anesthetic doses of ketamine [15], a common measure of unconsciousness in rodents. We propose that the disappearance of the HFO at higher doses of ketamine comes from non-NMDAR effects antagonizing the NMDAR effects. We model the non-NMDAR effects of ketamine with another Hill-type function (figure 1B, dashed red line):

$$E_{nNDMAR} = \frac{E_{max} C_b^N}{EC_{50,-}^N + C_b^N} \tag{5}$$

where E_{nNDMAR} is the non-NMDAR effect, and $EC_{50,-}$ is the EC_{50} concentration of the non-NMDAR effect. The subscript $-$ denotes that in our model the non-NMDAR actions have an inhibitory effect on HFO power. Direct empirical evidence for using a sigmoid to model the non-NMDAR effects comes from *in vitro*, slice and *in vivo* studies. In vitro studies have shown that binding of ketamine to monoaminergic (dopamine D_2 and serotonin $5HT2_A$ receptors follow sigmoid curves [10, 13]. Whole–cell recordings in mice pre-frontal slices have also shown that inactivation of I_h currents by ketamine binding to HCN1 receptors follows a dose-dependent sigmoid curve [9, 14]. Evidence obtained *in vivo* has shown that the fraction of mice obtunded by ketamine follows a dose-dependent sigmoid curve, and that such sigmoid is displaced to the right in HCN1 knockout mice [9]. These pieces of evidence provided support for our assumption of a sigmoid model for the non-NMDAR actions of ketamine. Furthermore ketamine binding to D_2, $5HT2_A$, and HCN1 receptors occurs at higher concentrations of than those required to bind to the NMDA receptor. In summary higher amounts of ketamine are required to produce anesthesia and ketamine binding to non-NMDA receptors occurs at higher concentrations. Therefore we postulated that the non-NMDAR actions are responsible for HFO power attenuation and disappearance and used a sigmoid curve to model the non-NMDAR ac-

tions at higher concentration of ketamine.

Therefore the estimated effect of ketamine concentration on the HFO power, termed $HFO(C_b)$, is governed by the opposing effects that the non-NMDAR actions exert over the NMDAR action. We assume these opposing influences as the difference between the NMDAR and non-NMDAR actions, expressed as $HFO(C_b) = E_{NDMAR} - E_{nNDMAR}$, and obtain:

$$\begin{aligned} HFO(C_b) &= \frac{E_{max}C_b^N}{EC_{50,+}^N + C_b^N} - \frac{E_{max}C_b^N}{EC_{50,-}^N + C_b^N} \\ &= E_{max}C_b^N \left[\frac{EC_{50,-}^N - EC_{50,+}^N}{(EC_{50,-}^N + C_b^N)(EC_{50,+}^N + C_b^N)} \right] \end{aligned} \tag{6}$$

where $EC_{50,-} \geq EC_{50,+}$. This is a reasonable assumption because the affinity of ketamine for the NMDAR receptor is greater that any of the non-NMDAR affinities [10].

This difference interaction between NMDAR and non-NMDAR effects of ketamine (figure 1B) produces a non-monotonic PD function (figure 1C). This non-monotonic PD function is key to account for the non-linear relationship between ketamine concentration obtained from the PK model and the observed time course of HFO power. The combination of the compartmental PK model (equation 1) and the difference PD function (equation 6) produces the curve denoted as $HFO(C_b, t)$ (figure 1D, upper right panel). This is the estimated time course of the HFO power. Shortly after ketamine dosing, when the drug concentration is rising in the brain, $HFO(C_b, t)$ displays a peak (figure 1D, triangle). This is the point of maximum effect given by HFO_{max}. As ketamine concentration keeps on rising and reaches the maximum, the estimated $HFO(C_b, t)$ displays a dose-dependent trough (figure 1D, circle). The higher the concentration of ketamine in the brain at the maximum point, the deeper the trough will be in $HFO(C_b, t)$. Then, ketamine concentration C_b starts to decay, and the trough is followed by a slow rise and decay in $HFO(C_b, t)$ (figure 1D, square).

3 Methods

3.1 Ethics Statement

All animal work has been conducted in accordance to federal, state, and local regulations, and following NIH guidelines and standards. The protocol #0511-044-14 was approved by the Institutional Animal Care and Use Committee at the Massachusetts Institute of Technology.

3.2 Animals and surgical procedures:

Six Sprague-Dawley rats (Charles River, Cambridge, MA), weighing between 400–600 g, were used in all experiments. Rats were individually caged under a 12/12 light/dark cycle, and kept in a humidity- and temperature-controlled room. Electrode implantation was performed under continuous 2% isoflurane anesthesia. Buprenorphine i.p. (0.01 mg/kg) was given as pre-emptive analgesic, and twice a day for two days after surgery for post-surgical analgesia. When the surgical plane was achieved, eight craniotomies were made in the following locations: 2.5 mm AP and ±1.2 mm ML, -1 mm AP and ±2 mm ML, -3.8 mm AP and ±2 mm ML, and -5.6 mm AP and ±2 mm ML (figure 2A). These locations were chosen to sample simultaneously from several cortical sites. The electrodes were made with two strands tungsten wire (12 μm, California Fine Wire, Grover Beach, CA). The strands were twisted using an automated wire twister (Open-ephys, Cambridge, MA), and held together by heating the insulation. One end of the electrodes was connected to an Electrode Interface Board EIB HS-16 (Neuralynx, Bozeman, MT) using gold pins. The other end of the electrodes was placed in contact with the dural surface through each craniotomy, and held in place with dental cement (C&B Metabond, Parkell, Edgewood, NY). Two additional craniotomies were made over the cerebellum, left and right of the midline, to implant the reference and ground screws (figure 2A).

3.3 Drugs:

Stock solutions of ketamine and MK-801 (Sigma-Aldrich, Natick, MA) were prepared by dissolving the drugs in sterile phosphate buffer saline (PBS, Boston BioProducts, Ashland, MA) under sterile conditions. Ketamine stock concentration was 200 mg/mL, and MK-801 stock concentration was 1 mg/mL. The stock solutions were diluted as needed under sterile conditions, on the same day that the injection was performed. Two doses of ketamine (30 and 80 mg/kg), and two doses of MK-801 (0.05 and 0.1 mg/kg) were injected i.p., in a volume of 1 mL/kg. The doses were chosen based on previous literature [17, 25, 26]. An injection of sterile PBS was used as a handling control. The five injections (two doses of ketamine, two doses of MK-801, and one PBS injection) were delivered to each animal in random order (figure 2B).

3.4 Behavioral testing and data acquisition:

For the electrophysiological recordings, the animals were placed in a custom-made circular recording chamber (35 cm diameter x 34 cm height) at least seven days after surgery. The ECoG was recorded at a sampling frequency of 2,713 Hz using a DigitalLynx system and Cheetah recording software (Neuralynx, Bozeman, MT). The ECoG signals were band-pass filtered between 0.1 Hz and 500 Hz, and referenced to the cerebellar skull screw. The

animals were habituated to the recording setup for two days before the first injection. Video was recorded continuously through all of the experiments, for posterior assessment of behavioral events such as movements, duration of injection procedure, and loss and recovery of the righting reflex. A baseline period of 30 minutes was recorded before the injection of each drug. The loss of righting reflex (LORR), a common measure of loss of consciousness for rodents [27], was tested every 30 seconds after the injection of the highest dose of ketamine (80 mg/kg), by quickly placing the rat in the supine position. Complete LORR was declared if the rat was not able to return to normal standing position within 30 seconds [28]. After LORR was declared, the rats were left in the supine position until they spontaneously recovered the righting reflex.

3.5 Signal processing and analysis:

The signals were pre-processed by removing linear trends and 60 Hz pick-up. After these pre-processing steps, the signals were downsampled to a sampling frequency of 1356 Hz. Spectrograms were computed between 100 and 200 Hz, in epochs of 10 seconds with 25% overlap, at a resolution of 0.4 Hz. All spectrograms were standardized to a period of 10 minutes of awake baseline. This period was identified based on video recordings and wide-band spectral features [29]. Ketamine and MK-801 are know to distribute unevenly across the brain [30, 31] which may influence the observed instantaneous HFO power [17] and frequency [19]. Therefore, before computing the HFO power, median spectrograms for each rat and treatment were obtained from all recording sites. The time course of the HFO power was then computed as the integral over time of the median spectrogram, in the 130–160 Hz frequency range. The HFO power was subsequently smoothed using a robust lowess procedure with a window span of 28 seconds [32]. Before fitting the model, the HFO power was standardized between 0 and 1 by subtracting its minimum value, and dividing by its maximum value. All signal processing was performed with MATLAB (The Mathworks, Natick, MA) and the Chronux toolbox [33].

3.6 Statistics and modeling procedure:

The compartmental model (equations 1, 2, and 3) and the PD function (equation 6) were fitted to the time course of the HFO power after the two doses of ketamine and the two doses of MK-801. To estimate the PK-PD parameters, k_{ab}, k_{ba}, k_{el} (equation 2), $EC_{50,+}$, $EC_{50,-}$, HFO_{max}, and N (equation 6), the model was fitted using a nonlinear least-squares method [34, 35]. During the fitting procedure, the quantity that was minimized was the weighted sum of squares of the error ($wSSE$) defined by:

$$wSSE = \sum w \cdot (HFO(C_b, t) - HFO)^2 \tag{7}$$

where the weighting function, w, placed most of the weight of the fit on the first two-thirds of the complete recording session. The weighting function, w, was defined as:

$$w = 1 - \frac{t^{12}}{(n - n/3)^{12} + t^{12}} \tag{8}$$

where t is the vector of timestamps in seconds, and n is the duration of the recording session in samples. The fitting procedure was implemented in MATLAB. Ten repetitions of the fitting procedure were carried out for the HFO power recorded from each rat at each dose, using initial conditions that were randomly generated .

The quality of each fit was assessed using the adjusted coefficient of determination R^2:

$$R^2 = 1 - \frac{wSSE}{wSST} \tag{9}$$

where $wSST$ is the weighted total sum of squares, defined by

$$wSST = \sum w \cdot \left(HFO - \overline{HFO}\right)^2 \tag{10}$$

where $\overline{HFO}$ is the mean of the observed HFO power. The fit with the maximum R^2, chosen from the ten repetitions of the fitting procedure for each rat and each dose, was considered as the best fit.

To compare the rate constants, k_{ab}, k_{ba}, and k_{el}, obtained from our model with the constants from published PK data, we applied the same procedure as described earlier. We fitted equations 1, 2 and 3 to the published PK data was obtained from Palenicek et al. [36], and it was extracted using the software PlotDigitizer v2.6.6. The rate constants reported in the text were selected by using the higher R^2 criteria. Confidence intervals for the mean were obtained by using a non-parametric bootstrap procedure.

In order to assess whether the instantaneous power of the HFO induced by MK-801 is also has a triphasic shape, we fitted the PK-PD model to it and compared the R^2 values obtained to those obtained by the fit to the ketamine-induced HFO. Because in non-linear fits the R^2 values can sometimes be greater than one, we standardized all the R^2 values to the maximum R^2 value obtained from the ten repetitions of the fit for each rat. The R^2 values were compared using repeated measures ANOVA test across all subjects. All statistical procedures were carried out using SPSS (IBM, Armonk, NY) or MATLAB (The Mathworks, Natick, MA).

4 Results

4.1 Behavioral differences after dosing of NMDAR antagonists.

The drugs were administered in a randomized design. A total of five injections were performed in each rat (n = 6). Injections of both NMDAR antagonists, ketamine and MK-801, produced hyperactivity and stereotyped behaviors in all rats, as has been previously described [37]. However, only a 80 mg/kg dose of ketamine produced LORR. The mean LORR onset was 3.5 ± 0.94 min (mean ± SEM), and a had mean duration of 61.11 ± 14.24 min. These results demonstrate that the chosen high dose of ketamine was enough to produce loss consciousness, and therefore, will provide a useful contrast to the low ketamine dose (30 mg/kg) to test our hypothesis that the HFO power is non-linearly modulated by ketamine concentration.

4.2 The HFO as an effect of NMDAR antagonism.

The HFO produced by both NMDAR antagonists has small amplitude, but can be observed in the raw trace (figure 2C). The HFO becomes more evident after band-pass filtering between 130–160 Hz (figure 2D). The HFO was observed in all the subjects (n = 6) in all the cortical regions recorded (8 locations per subject) and after both doses of either ketamine or MK-801 (figure 3A–E). Only the injection of 0.05 mg/kg of MK-801 did not produced the HFO in the most posterior electrodes. These regional lack of effect was only observed in a subset of the animals (2/6). The HFO was not observed after the injection of PBS, although power in the wide frequency band between 130–160 Hz was occasionally observed due to movement artifacts (figure 3A). These results suggests that the HFO is reproducible across rats after dosing of either NMDAR antagonist.

The HFO produced by NMDAR antagonists appeared in the frequency band between 130–160 Hz. It constitutes a well defined spectral peak (figure 2E) with an average frequency of 143.33 ± 0.51 Hz. A Kruskal-Wallis ANOVA yielded no evidence of the HFO average frequency differing between ketamine or MK-801 dosing (ket30 = 144.75 ± 1.24 Hz; ket80 = 140.95 ± 1.85 Hz; mk005 = 142.78 ± 1.64 Hz; mk01 = 144.83 ± 0.91 Hz; $\chi^2_{3,20} = 2.92$, p = 0.40) (figure 2F). These results suggest that the nature of the HFO is the same after dosing of either NMDAR antagonists.

4.3 Time course of HFO power after ketamine dosing.

The time course of HFO power observed after dosing of MK-801 displays a single, slow rise and decay (figure 3E and D, and figure 4A and B). The brief period of higher power right after the injection is likely due to the movement artifacts that resulted from the

injection procedure. However, the time course of HFO power after ketamine dosing is characteristically different from the time course of HFO power after MK-801 dosing. The time course of HFO power displayed a triphasic profile.

The first phase of the time course of HFO power was characterized by a initial peak in HFO power profile. This peak typically occurred within the first three minutes after the injection (figure 3C, and 4A and B), as shown in previous reports [17]. The peak HFO power during this phase was taken as the maximum value during the first three minutes after dosing. When testing for differences in peak HFO power during this first phase, the power observed after the injection of 30 (2.76 ± 0.28) and 80 (2.64 ± 0.21) mg/kg of ketamine was significantly greater than the power after the injection of PBS (1.22 ± 0.07). The power after the injection of MK-801 was not significantly greater than PBS during this period (mk005 = 1.36 ± 0.13; mk01 = 1.52 ± 0.10. $\chi^2_{4,25} = 21.76$, $p \ll 0.001$, Tukey's HSD post-hoc test) (figure 4C).

The second phase of the time course of HFO power consisted of a power trough. This trough was transient after the lower ketamine dose (30 mg/kg) (figure 4A), and more sustained after the higher ketamine dose (figure 4B). The duration of this power trough was qualitatively coincident with LORR. To assess whether the power trough reached the control (PBS) power levels, we tested for differences in minimum power during the first six minutes after dosing of either NMDAR antagonists or PBS. The minimum power here was taken as the minimum power value during the first six minutes. A Kruskal-Wallis ANOVA yielded no evidence of differences in power after dosing any of the NMDAR antagonists or PBS (PBS = 0.73 ± 0.06; ket30 = 1.35 ± 0.22; ket80 = 0.95±0.20; mk005 = 0.72±0.06; mk01 = 0.93±0.12. $\chi^2_{4,25} = 6.16$, p = 0.1872, Tukey's HSD post-hoc test).

The third phase of the time course of HFO power consisted of a slow increase and posterior decrease. This third phase had a shorter duration after the low dose (figure 3A) compared to its duration after the higher dose (figure 4B). This is likely due to the longer time ketamine remains in the brain subsequent to when a higher dose is administered. The observed differences in time course of the HFO power cannot be attributed to difference in handling during injection of the drugs and PBS. The mean duration of the injection procedure was 34.88 ± 0.99 seconds, from the moment the animals were removed from the recording chamber until they were returned. A two-way ANOVA yielded no evidence of a difference between the duration of injection across the different treatments ($F_{4,20} = 0.37$, p = 0.83), or subjects ($F_{5,20} = 0.78$, p = 0.57).

To account for the possibility that the first power peak is a result of movement and handling artifacts caused by the animal's reaction to the injection procedure, we measured the difference between the power peak and the power trough for each rat at each condition. The mean ± s.e.m. values in each group are: PBS = 0.41±0.05; ket30 = 1.33

$\pm$ 0.14; ket80 = 1.65 $\pm$ 0.24; mk005 = 0.61 $\pm$ 0.12; mk01 = 0.55 $\pm$ 0.04. If the HFO power peak is merely a handling artifact, there should be no differences in this quantity across treatments. A Kruskal-Wallis ANOVA yields strong evidence of difference across the groups ($\chi^2_{4,25}$ = 19.75, p = 0.001). A post-hoc pairwise comparisons yields strong evidence that the peak-trough power difference after dosing of 30 mg/kg and 80 mg/kg of ketamine are larger than the peak-trough power difference after dosing of PBS and 0.05 mg/kg of MK-801 ($p_{PBS-ket30}$ = 0.002; $p_{PBS-ket80}$ = 0.001; $p_{ket30-mk005}$ = 0.006; $p_{ket80-mk005}$ = 0.002. Tukey's HSD post-hoc test). The same test yields weak evidence of difference between 80 mg/kg of ketamine and 0.1 mg/kg of MK-801 in the peak-trough power difference ($p_{ket80-mk01}$ = 0.022. Tukey's HSD post-hoc test). However, there is no significant difference between 30 mg/kg of ketamine and 0.1 mg/kg of MK-801 ($p_{ket30-mk01}$ = 0.053).

These results suggest that while the HFO that is produced by the selective NMDAR antagonist, MK-801, constitutes a continuous effect of NMDAR antagonism, the HFO after ketamine was discontinued for a period of time in a dose dependent manner. However, we have not completely ruled out the possibility that MK-801, at the higher dose, does in fact produce a triphasic-shaped HFO instantaneous power. As described in the next two sections, we further test for this possibility by fitting the model to the HFO power time course after dosing each of the non-NMDAR antagonists.

4.4 The PK-PD model fits well the HFO time course after ketamine dosing

The previous results show that the HFO power constitutes an appropriate surrogate for ketamine effects. We then tested the proposed PK-PD model on the time course of HFO power obtained from each individual rat, after each dose of ketamine. While each individual HFO power displayed the triphasic profile observed in the average (figure 4), the actual time course was variable across animals (figure 5B and 6B, green lines). Ten repetitions of the fitting procedure were run for each rat and ketamine dose, and the fit with the maximum R^2 was chosen for each animal (figure 5A and 6A). The extent of convergence was variable, but the parameters of the PK-PD model with the maximum R^2 provided good fits for both the lower (Table 1) and the higher ketamine doses (Table 2). The estimated fit with these parameters can be seen in figure 5B and figure 6B (red line). The maximum values of R^2 obtained after the injection of 30 mg/kg were above 0.5 for all animals (0.74 $\pm$ 0.04) (Table 1). The model was robust to the movement artifacts, even when they were present during the main time course of HFO (figure 5B, rat 6). The maximum values of R^2 for the fits to the higher ketamine dose (80 mg/kg) are all above 0.5 (0.81 $\pm$ 0.05). The model again displays robustness to movement artifacts, which in this case typically occurred after the recovery of righting reflex (figure 6B, rat 2). The

R^2 values were not different between ketamine doses (Mann-Whitney test, U = 34, p = 0.48,), providing evidence that the quality of the fit was the same for both low and high ketamine doses.

In order to compare the rate values obtained from the model with known PK data for ketamine in the brain, we applied the PK fitting procedure (equations 1, 2 and 3) to the published PK data from Palenicek et al [36]. This data set corresponds to brain concentration of ketamine after the i.p. injection of 30 mg/kg of ketamine in rats. As done previously, we chose the rates obtained from the fit with the highest R^2 value (0.93) out of 10 repetitions of the fitting procedure. The rate value obtained for $k_{el} = 0.0786$ min^{-1}, and is within the range of rates values obtained from the fits to the HFO power in the 6 rats (table 1). Furthermore, it lies within the 95% confidence intervals (CI) of the mean ($\mu = 0.0415$ min^{-1}, CI = [0.0211 min^{-1} 0.1172 min^{-1}]). The rate value obtained for $k_{ab} = 0.0985$ min^{-1}, which is also within the range of rates values obtained from the fits to the HFO power in the six rats (table 1). This rate value is also within the 95% CI of the mean ($\mu = 0.1809$ min^{-1}, CI = [0.0921 min^{-1} 0.2496 min^{-1}]). However, the value obtained for the rate $k_{ba} = 0.0787$ min^{-1} was not within the range of values obtained from fit to the HFO (table 1). The rates to fit the HFO power were obtained by jointly fitting the PK and PD models, and the discrepancy could be due to the NMDAR antagonism that some ketamine metabolites have.

4.5 The PK-PD model does not fit well the HFO time course after MK-801 dosing

The assumptions of the proposed PK-PD model imply that a clean NMDAR antagonists should not produce triphasic HFO power. However, figure 2A and B show that there is a rise in HFO power after MK-801 and PBS injection. We have attributed this to movement and handling artifacts introduced in the electrophysiological recordings. While the peak-trough power differences confirmed this assumption for most of the groups, the statistical analysis, in section 4.3, did not provide evidence of a difference in the peak-trough power between the lower dose of ketamine and the higher dose of MK-801. In order to further test that MK-801 does not produce a triphasic HFO, we applied the fitting procedure under the same conditions to the HFO time course after dosing of both doses of MK-801. A repeated measures ANOVA over the corrected R^2 values between the lower dose of ketamine (0.75 ± 0.05), the lower dose of MK-801 (0.27 ± 0.05), the high dose of ketamine (0.79 ± 0.03) and the high dose of MK-801 (0.40 ± 0.04) yields strong evidence of the R^2 values obtained for MK-801 are lower than those obtained for ketamine ($F_{(3,36)} = 37.47$, $p \ll 0.001$). The post-hoc test yields strong evidence that the R^2 values obtained from fits to low and high dose of ketamine are higher than those obtained from low and high dose of MK-801 (all p-values $\ll 0.001$, Tukey's HSD test). The post-hoc test also yields

strong evidence that the R^2 values obtained from low and high ketamine and from low and high dose of MK-801 are not significantly different ($p_{ket30-ket80} = 0.89$, $p_{mk005-mk01} = 0.14$, Figure 7).

5 Discussion

Our study provides a PK-PD model to relate the NMDAR and non-NMDAR effects of ketamine to the time course of HFO power observed in the rodent ECoG (figure 1 and equation 6). The model is based on the difference interaction between NMDAR and non-NMDAR effects of ketamine. To test the model, we continuously recorded HFO from the cortical surface of freely moving rats (figure 3A and C), after injections of ketamine and MK-801. We showed that the HFO frequency after ketamine dosing it is not different from the HFO frequency after MK-801 dosing (figure 3E and F). However, the HFO power produced by ketamine differs in its time course from the HFO power produced by MK-801 (figures 3 and 4). We showed that the estimated PK-PD model (equation 6) fits well the time course of ketamine-induced HFO power, for both low and high ketamine doses (figures 5 and 6), while it does not produce a good fit to the MK-801-induced HFO power, at any of the doses tested.

5.1 Rationale behind the PK model:

Three-compartment models are typically used for i.p. pharmacokinetic studies [38]. However, there is evidence that ketamine may be actively transported into the brain, because studies that have simultaneously measured ketamine concentration in plasma and brain found that the brain concentration was higher than the plasma concentration at every time measured [36, 38]. Passive diffusion of the drug across compartments will not realistically describe the measured concentrations of ketamine in the plasma and in the brain. We have chosen a minimal two-compartmental model in which the ancillary compartment could be considered as the merger between the peritoneal space and the central compartment. We demonstrated that this model could account for the observed time course of the HFO power across two different ketamine doses. The values of the rate constants have not been published, and therefore we cannot directly compare the values obtained by fitting our model. However, we have fitted the proposed PK model to published data for ketamine concentration in the rat brain [36], and found that the values of two of the rate constants (k_{el} and k_{ab}) are consistent with the values obtained by fitting the complete PK-PD model to the HFO instantaneous power.

5.2 Rationale behind PD model:

The HFO power is not linearly related to the ketamine brain concentration (figure 4). Rather, the HFO power shows a dose-dependent decrease in power shortly after ketamine dosing, which results in a curve that has a fast rise and decay, followed by a second, slower rise and decay (figure 3). We reasoned a non-monotonic PD model could account for the observed HFO power time course. We built the PD model based on two monotonic Hill-type sigmoids. The NMDAR sigmoid (figure 1B, continuous line) accounts for the time course of HFO power due to the non-NMDAR actions. The key insight is that the non-NMDAR actions can be represented by a second sigmoid (figure 1B, dashed line). The non-monotonic HFO response results from the difference between the two sigmoids (figure 1C).

The PD model hinges on the assumption that the disappearance of the HFO is due to the non-NMDAR actions of ketamine, and that this effect gives rise to the triphasic HFO shape. If this is true, then a pure NMDAR antagonist, such as MK-801, should not produce a triphasic HFO. However, the data presented in figures 4A and B suggest that MK-801 could also have a short, single peak followed by trough, giving rise to a triphasic shape. However, when fitting the PK-PD model to the HFO time course induced by MK-801, we found that the quality of the fits are consistently worst than those obtained for ketamine (figure 7). These results further support for our hypothesis for the non-NMDAR actions of ketamine are responsible for the HFO disappearance, and therefore for the proposed PD model.

It is not yet clear which of the non-NMDAR actions of ketamine accounts for HFO disappearance. The HFO was first identified in the nucleus accumbens [15], but local injections of dopamine D_1 and D_2 antagonists in the nucleus accumbens do not affect the HFO power [39]. It is possible that the attenuation in HFO power could be due to the actions of ketamine on HCN1 receptors. Ketamine inhibits HCN1-mediated I_h currents at an EC_{50} of 15 μM [9] while it blocks NMDAR channels at EC_{50} of 9 μM [7]. The fact that the HFO disappears at anesthetic concentrations of ketamine [15] suggests that the higher dose necessary to produces loss of consciousness and to inhibit HCN1-mediated currents could also be related to the attenuation in HFO power.

5.3 The HFO as a surrogate for NMDAR actions:

Part of the challenge of creating PK-PD models lies in finding appropriate surrogate effect for both the PK and PD aspects of the drug. An appropriate surrogate effect should be objective, reproducible, continuous, and relevant to the pharmacological actions of the drug.

Electrophysiological measures are objective and can be considered reproducible and continuous for drugs with actions in the central nervous system [40]. In particular, we have shown here that the HFO is continuous (figures 3 and 4), and reproducible (figure 2C, E and F). Other studies have also used different ECoG measures to develop PK-PD models in rodents [41] and humans [42].

The relationship between HFO and NMDAR antagonism has also been previously established [15, 20, 43]. We have used a specific NMDAR antagonist, MK-801, to further establish that the HFO power due to specific NMDAR antagonism is dose-dependent, and that exhibits a single raise and decay over time in the absence of other pharmacological actions. Therefore, the HFO relates directly to the main pharmacological action of ketamine, and fulfills the criteria for an appropriate PK-PD surrogate effect.

5.4 Possible effects of ketamine metabolites:

Norketamine, the primary metabolite of ketamine, is an NMDAR antagonist [44] with analgesic and anesthetic properties [45–47] that is known to cross the blood-brain barrier in rats [36,38]. It is possible that norketamine will have a favorable effect on the strength of the HFO instantaneous power, given norketamine's actions as an NMDAR antagonist. However, to our knowledge, there is no study assessing the electrophysiological effects of norketamine.

Furthermore, the pharmacokinetics of norketamine in the rodent brain have not yet been elucidated. Two studies have addressed the joint pharmacokinetics of ketamine and norketamine in rats [36, 38]. Both studies agreed that the norketamine's concentration in the rat's plasma is higher and that it has a longer half-life than ketamine. However, their results differ regarding norketamine's concentration in the brain. One study reported that norketamine has a higher peak concentration than that of ketamine, but has a similar half-life [36]. The other study reported that norketamine has a lower peak concentration, but has a longer half-life than ketamine [38]. These discrepancies make it difficult to hypothesize the role that norketamine could play in our model. For example, if norketamine lasts longer in the brain than ketamine, it could extend the duration of the HFO. However, if only the peak concentration of norketamine is higher, its HFO-promoting effects could be attenuated by the non-NMDAR actions of ketamine, which is a central point of our model. Further experiments should be conducted to clarify the relationship between the HFO power, norketamine, and the role it could play in our model.

5.5 Origin of the HFO:

The origin of the HFO has not been established. The HFO has been recorded in the cortex [20], motor circuits of the basal ganglia [17], nucleus accumbens [15], and hippocampus [48]. Narrow band oscillations such as the HFO are unlikely to be an artifact [29]. It has been proposed that the HFO originates from monopolar sources in the nucleus accumbens [43]. However, it is unknown if the HFO passively propagates to cortex and the other areas where has been recorded [17]. Regardless of its origin, the HFO power correlates with hyperactivity [15], and our findings and those from previous studies suggest that it results from both competitive and non-competitive NMDAR antagonism [20].

5.6 Relationship to previous work:

We have applied the concept of difference interaction to different pharmacological actions within the same drug. The same concept has been used to model opposing interactions between different drugs. For example, interactions between cholinergic agonists and antagonists drugs in clinical trials of Alzheimer therapies [49], and studies of the different effects of the components of a racemic mixture of ketamine. The same study also showed that the PK of the individual stereoisomers was not different from the PK of the racemic mixture. These results simplify the analysis of the PK-PD properties of ketamine racemic mixture, which is the form commonly used in the clinic and in research, and the one we have used in this study.

5.7 Future directions:

The HFO has been shown to be directly related to hyperactivity [15], and therefore, the proposed model could also be used to analyze behavior in animal models [37]. Another application could be to study the PK-PD properties of other drugs with several pharmacological actions that might become relevant at different concentrations, such as several psychiatric drugs.

While the proposed PK-PD model works well for two doses of ketamine and a variety of HFO time courses across individuals, the model did not accurately reproduce the HFO power after the low dose of ketamine in one of the subjects (figure 5B, rat 4). In this case, the time course of HFO power is much shorter than the other cases. This kind of variability is expected after i.p. injections. Handling the animal to deliver the i.p. injection also introduces wide-band artifacts that can leak power into the initial phase of the HFO (figure 4A, B and C). This poses a fitting problem, because the HFO does not always start from zero power, a requirement from the PD equation. Both issues could be

addressed by delivering ketamine through intravenous injections.

5.8 Conclusions:

We have postulated and tested a model that can explain the time course of the HFO power based on the PK-PD properties of ketamine. At low doses, ketamine has a wide range of uses such as analgesic, antidepressive, model for schizophrenia, and drug of abuse. At higher doses, ketamine can be used for safe induction of loss of consciousness, because it does not depress respiratory function [50]. By incorporating the different pharmacological actions of ketamine into a single PK-PD model, and establishing the HFO as a good surrogate effect for the main pharmacological action of ketamine, our study suggests that this wide range of effects could be brought about by different pharmacological actions of ketamine, that are relevant at different drug concentrations. Tracking the HFO could be useful in other experimental settings in rodents to study the wide and divergent range of effects that ketamine has.

Acknowledgments:

This work has been supported by the National Institute of Health Pioneer Award DP1-OD003646 to Emery N. Brown; the Career Award at the Scientific Interface from the Burroughs-Wellcome Fund to ShiNung Ching; the National Institute of Health Grant 5R01MH061976 to Matthew A. Wilson, and the National Institute of Health New Innovator Award DP2-OD006454 to Patrick L. Purdon.

References

1. Laurido C, Pelissier T, Pérez H, Flores F, Hernández A (2001) Effect of ketamine on spinal cord nociceptive transmission in normal and monoarthritic rats. Neuroreport 12: 1551–1554.

2. Wurtman RJ (2010) Fibromyalgia and the complex regional pain syndrome: similarities in pathophysiology and treatment. Metabolism: Clinical and Experimental 59 Suppl 1: S37–40.

3. Canet J, Castillo J (2012) Ketamine: a familiar drug we trust. Anesthesiology 116: 6–8.

4. Zarate CA, Singh JB, Carlson PJ, Brutsche NE, Ameli R, et al. (2006) A randomized trial of an n-methyl-d-aspartate antagonist in treatment-resistant major depression. Archives of General Psychiatry 63: 856–864.

5. Javitt DC (2007) Glutamate and schizophrenia: phencyclidine, n-methyl-d-aspartate receptors, and dopamine-glutamate interactions. International Review of Neurobiology 78: 69–108.

6. Morgan CJA, Curran HV, the Independent Scientific Committee on Drugs (ISCD) (2012) Ketamine use: a review. Addiction 107: 27–38.

7. MacDonald JF, Miljkovic Z, Pennefather P (1987) Use-dependent block of excitatory amino acid currents in cultured neurons by ketamine. Journal of Neurophysiology 58: 251–266.

8. Kohrs R, Durieux ME (1998) Ketamine: teaching an old drug new tricks. Anesthesia & Analgesia 87: 1186–1193.

9. Chen X, Shu S, Bayliss DA (2009) HCN1 channel subunits are a molecular substrate for hypnotic actions of ketamine. The Journal of neuroscience: the official journal of the Society for Neuroscience 29: 600–609.

10. Kapur S, Seeman P (2002) NMDA receptor antagonists ketamine and PCP have direct effects on the dopamine d(2) and serotonin 5-HT(2)receptors-implications for models of schizophrenia. Molecular Psychiatry 7: 837–844.

11. Finck AD, Ngai SH (1982) Opiate receptor mediation of ketamine analgesia. Anesthesiology 56: 291–297.

12. Hirota K, Hashimoto Y, Lambert DG (2002) Interaction of intravenous anesthetics with recombinant human m1-m3 muscarinic receptors expressed in chinese hamster ovary cells. Anesthesia and analgesia 95: 1607–1610, table of contents.

13. Seeman P, Kapur S (2003) Anesthetics inhibit high-affinity states of dopamine d2 and other g-linked receptors. Synapse (New York, NY) 50: 35–40.

14. Zhou C, Douglas JE, Kumar NN, Shu S, Bayliss DA, et al. (2013) Forebrain HCN1 channels contribute to hypnotic actions of ketamine. Anesthesiology 118: 785–795.

15. Hunt MJ, Raynaud B, Garcia R (2006) Ketamine dose-dependently induces high-frequency oscillations in the nucleus accumbens in freely moving rats. Biological Psychiatry 60: 1206–1214.

16. Hunt MJ, Garcia R, Large CH, Kasicki S (2008) Modulation of high-frequency oscillations associated with NMDA receptor hypofunction in the rodent nucleus accumbens by lamotrigine. Progress in Neuro-Psychopharmacology & Biological Psychiatry 32: 1312–1319.

17. Nicolás MJ, López-Azcárate J, Valencia M, Alegre M, Pérez-Alcázar M, et al. (2011) Ketamine-induced oscillations in the motor circuit of the rat basal ganglia. PloS one 6: e21814.

18. Hunt MJ, Falinska M, Kasicki S (2010) Local injection of MK801 modifies oscillatory activity in the nucleus accumbens in awake rats. Journal of Psychopharmacology (Oxford, England) 24: 931–941.

19. Olszewski M, Piasecka J, Goda SA, Kasicki S, Hunt MJ (2013) Antipsychotic compounds differentially modulate high-frequency oscillations in the rat nucleus accumbens: a comparison of first- and second-generation drugs. The international journal of neuropsychopharmacology / official scientific journal of the Collegium Internationale Neuropsychopharmacologicum (CINP) 16: 1009–1020.

20. Phillips KG, Cotel MC, McCarthy AP, Edgar DM, Tricklebank M, et al. (2011) Differential effects of NMDA antagonists on high frequency and gamma EEG oscillations in a neurodevelopmental model of schizophrenia. Neuropharmacology .

21. Ching S, Liberman MY, Chemali JJ, Westover MB, Kenny J, et al. (2013) Real-time closed-loop control in a rodent model of medically induced coma using burst suppression. Anesthesiology .

22. Liberman MY, Ching S, Chemali J, Brown EN (2013) A closed-loop anesthetic delivery system for real-time control of burst suppression. Journal of Neural Engineering 10: 046004.

23. Shanechi MM, Chemali JJ, Liberman M, Solt K, Brown EN (2013) A brain-machine interface for control of medically-induced coma. PLoS Comput Biol 9: e1003284.

24. Holford NH, Sheiner LB (1982) Kinetics of pharmacologic response. Pharmacology & Therapeutics 16: 143–166.

25. Wood J, Kim Y, Moghaddam B (2012) Disruption of prefrontal cortex large scale neuronal activity by different classes of psychotomimetic drugs. The Journal of Neuroscience 32: 3022–3031.

26. Quirk MC, Sosulski DL, Feierstein CE, Uchida N, Mainen ZF (2009) A defined network of fast-spiking interneurons in orbitofrontal cortex: responses to behavioral

contingencies and ketamine administration. Frontiers in Systems Neuroscience 3: 13.

27. Kleitman N (1957) Sleep, wakefulness, and consciousness. Psychological bulletin 54: 354–359; discussion 360.

28. Petrenko AB, Yamakura T, Fujiwara N, Askalany AR, Baba H, et al. (2004) Reduced sensitivity to ketamine and pentobarbital in mice lacking the n-methyl-d-aspartate receptor GluR1 subunit. Anesthesia & Analgesia 99: 1136–1140.

29. Scheffer-Teixeira R, Belchior H, Leo RN, Ribeiro S, Tort ABL (2013) On high-frequency field oscillations (>100 hz) and the spectral leakage of spiking activity. The Journal of neuroscience: the official journal of the Society for Neuroscience 33: 1535–1539.

30. Duncan GE, Miyamoto S, Leipzig JN, Lieberman JA (1999) Comparison of brain metabolic activity patterns induced by ketamine, MK-801 and amphetamine in rats: support for NMDA receptor involvement in responses to subanesthetic dose of ketamine. Brain Research 843: 171–183.

31. Lu J, Nelson LE, Franks N, Maze M, Chamberlin NL, et al. (2008) Role of endogenous sleep-wake and analgesic systems in anesthesia. The Journal of Comparative Neurology 508: 648–662.

32. Cleveland WS (1979) Robust locally weighted regression and smoothing scatterplots. Journal of the American Statistical Association 74: 829–836.

33. Mitra P, Bokil H (2007) Observed Brain Dynamics. Oxford University Press.

34. Nelder JA, Mead R (1965) A simplex method for function minimization. The Computer Journal 7: 308–313.

35. Lagarias JC, Reeds JA, Wright MH, Wright PE (1998) Convergence properties of the nelder–mead simplex method in low dimensions. SIAM Journal on Optimization 9: 112–147.

36. Palenicek T, Michaela F, Brunovsky M, Balikova M, Horacek J, et al. (2011) Electroencephalographic spectral and coherence analysis of ketamine in rats: correlation with behavioral effects and pharmacokinetics. Neuropsychobiology 63: 202–218.

37. Hakami T, Jones NC, Tolmacheva EA, Gaudias J, Chaumont J, et al. (2009) NMDA receptor hypofunction leads to generalized and persistent aberrant gamma oscillations independent of hyperlocomotion and the state of consciousness. PloS one 4: e6755.

38. Shaffer CL, Osgood SM, Smith DL, Liu J, Trapa PE (2014) Enhancing ketamine translational pharmacology via receptor occupancy normalization. Neuropharmacology 86: 174–180.

39. Matulewicz P, Kasicki S, Hunt MJ (2010) The effect of dopamine receptor blockade in the rodent nucleus accumbens on local field potential oscillations and motor activity in response to ketamine. Brain Research 1366: 226–232.

40. Stanski DR (1992) Pharmacodynamic modeling of anesthetic EEG drug effects. Annual Review of Pharmacology and Toxicology 32: 423–447.

41. Mandema JW, Kuck MT, Danhof M (1992) Differences in intrinsic efficacy of benzodiazepines are reflected in their concentration-EEG effect relationship. British journal of pharmacology 105: 164–170.

42. Schuttler J, Stanski DR, White PF, Trevor AJ, Horai Y, et al. (1987) Pharmacodynamic modeling of the EEG effects of ketamine and its enantiomers in man. Journal of Pharmacokinetics and Biopharmaceutics 15: 241–253.

43. Hunt MJ, Falinska M, Leski S, Wojcik DK, Kasicki S (2011) Differential effects produced by ketamine on oscillatory activity recorded in the rat hippocampus, dorsal striatum and nucleus accumbens. Journal of Psychopharmacology (Oxford, England) 25: 808–821.

44. Ebert B, Mikkelsen S, Thorkildsen C, Borgbjerg FM (1997) Norketamine, the main metabolite of ketamine, is a non-competitive NMDA receptor antagonist in the rat cortex and spinal cord. European Journal of Pharmacology 333: 99–104.

45. Zhao X, Venkata SLV, Moaddel R, Luckenbaugh DA, Brutsche NE, et al. (2012) Simultaneous population pharmacokinetic modelling of ketamine and three major metabolites in patients with treatment-resistant bipolar depression. British Journal of Clinical Pharmacology 74: 304–314.

46. Holtman Jr JR, Crooks PA, Johnson-Hardy JK, Hojomat M, Kleven M, et al. (2008) Effects of norketamine enantiomers in rodent models of persistent pain. Pharmacology Biochemistry and Behavior 90: 676–685.

47. Leung LY, Baillie TA (1986) Comparative pharmacology in the rat of ketamine and its two principal metabolites, norketamine and (Z)-6-hydroxynorketamine. Journal of Medicinal Chemistry 29: 2396–2399.

48. Caixeta FV, Cornlio AM, Scheffer-Teixeira R, Ribeiro S, Tort ABL (2013) Ketamine alters oscillatory coupling in the hippocampus. Scientific Reports 3.

49. Lockwood P, Ewy W, Hermann D, Holford N (2006) Application of clinical trial simulation to compare proof-of-concept study designs for drugs with a slow onset of effect; an example in alzheimer's disease. Pharmaceutical research 23: 2050–2059.

50. Ehrlichman R, Gandal M, Maxwell C, Lazarewicz M, Finkel L, et al. (2009) N-methyl-d-aspartic acid receptor antagonist-induced frequency oscillations in mice recreate pattern of electrophysiological deficits in schizophrenia. Neuroscience 158: 705–712.

Figure Legends

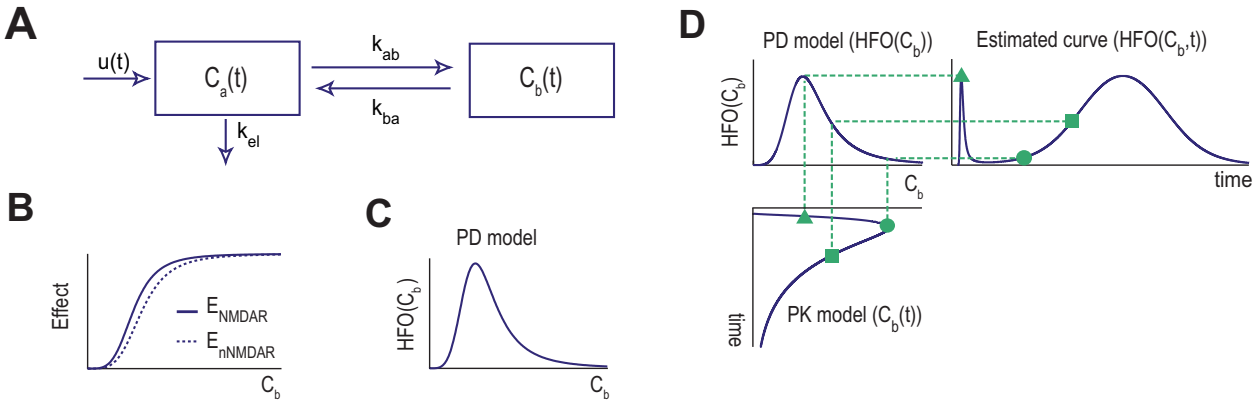

Figure 1. Schematics of PK-PD model and its relationship to HFO instantaneous power. (A) Two-dimensional compartment model, consisting of an ancillary compartment ($C_a(t)$) and the brain compartment ($C_b(t)$). The input is $u(t)$ and the rate constants are k_{ab}, k_{ba}, and k_{el}. (B) Individual PD curves representing the NMDAR (continuous line) and non-NMDAR (dashed line) actions of ketamine. (C) Non-monotonic PD model resulting from the difference between the NMDAR and non-NMDAR PD curves in (B). (D) Combining the PK (lower left panel) and PD (upper left panel) models produces the estimate for the time course of the HFO power, $HFO(C_b, t)$ (upper right panel). The three symbols connected by dashed lines exemplify the relationship between the PK model, the PD model, and the estimated curve $HFO(C_b, t)$ at three different points in time.

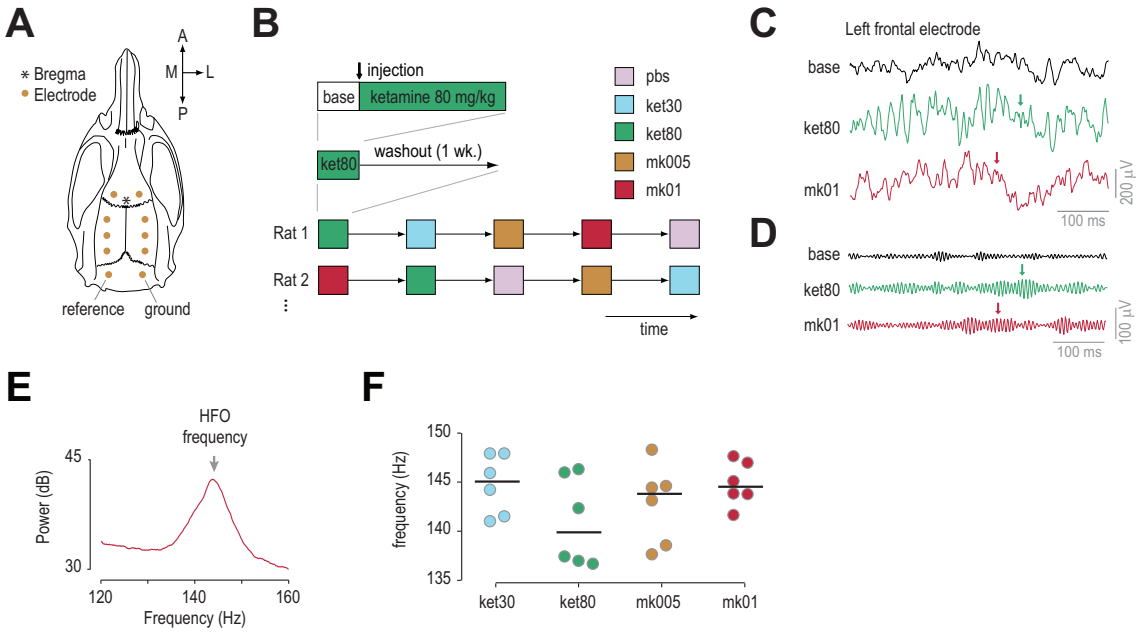

Figure 2. Experiment design, raw ECoG traces, and HFO frequency (A) Placement of recording, reference and ground electrodes in the rat skull (A: anterior; P: posterior; M: middle; L: lateral). (B) Experiment design: Thirty minutes of baseline (white area) were recorded before dosing, and then 3–4 hours after dosing (green colored area). One week of washout period was allowed between the five treatments: PBS; 30 mg/kg and 80 mg/kg of ketamine; 0.05 and 0.1 mg/kg of MK-801. The rats (n = 6) received the five treatments (colored boxes) in randomized order. (C) Example of raw ECoG traces, recorded during baseline (black), and one hour after dosing 80 mg/kg of ketamine (green) or 0.1 mg/kg of MK-801 (red) injection. (D) Same traces from (C), band–pass filtered between 130-160 Hz. The arrows point to periods with HFO. (E) Example spectrum a single frontal electrode after injection of 0.1 mg/kg of MK-801. The HFO constitutes a well defined spectral peak. The HFO frequency was considered as the frequency at peak power. (F) HFO frequency values across averaged across electrodes for every individual rat and treatment. No significant differences are observed (Kruskal-Wallis ANOVA p = 0.40).

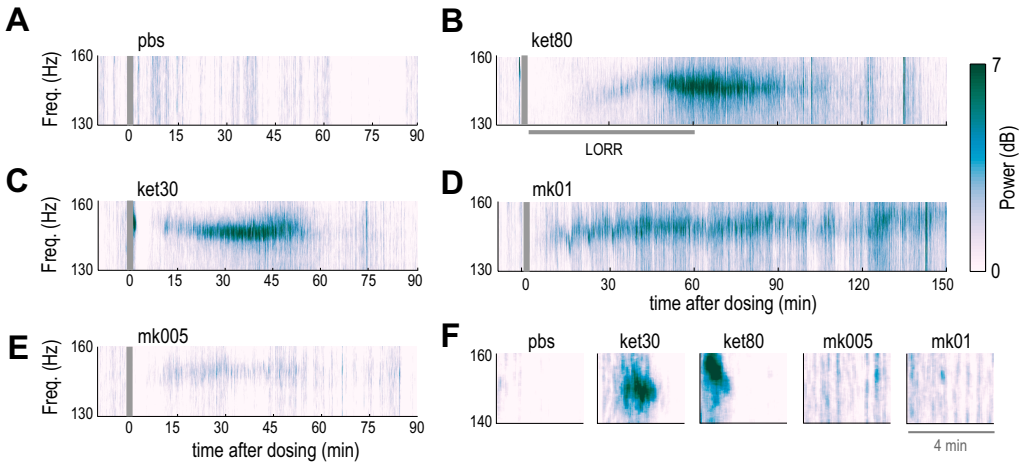

Figure 3. Example spectrograms after dosing of NMDAR antagonists. (A–E) Spectrograms averaged over all recording sites in a single rat. Dosing was performed at t = 0 (vertical line). Each spectrogram shows 10 minutes of baseline, and either 90 or 150 minutes after dosing of: (A) PBS; (B) 80 mg/kg of ketamine; (C) 30 mg/kg of ketamine; (D) 0.1 mg/kg of MK-801, and (E) 0.05 mg/kg of MK-801. The horizontal black line in (B) shows the duration of LORR. (F) Enlargement of the first 4 minutes of the spectrograms, showing the presence of a prominent HFO peak after the injection of both doses of ketamine. This peak is absent after the injections of PBS or MK-801.

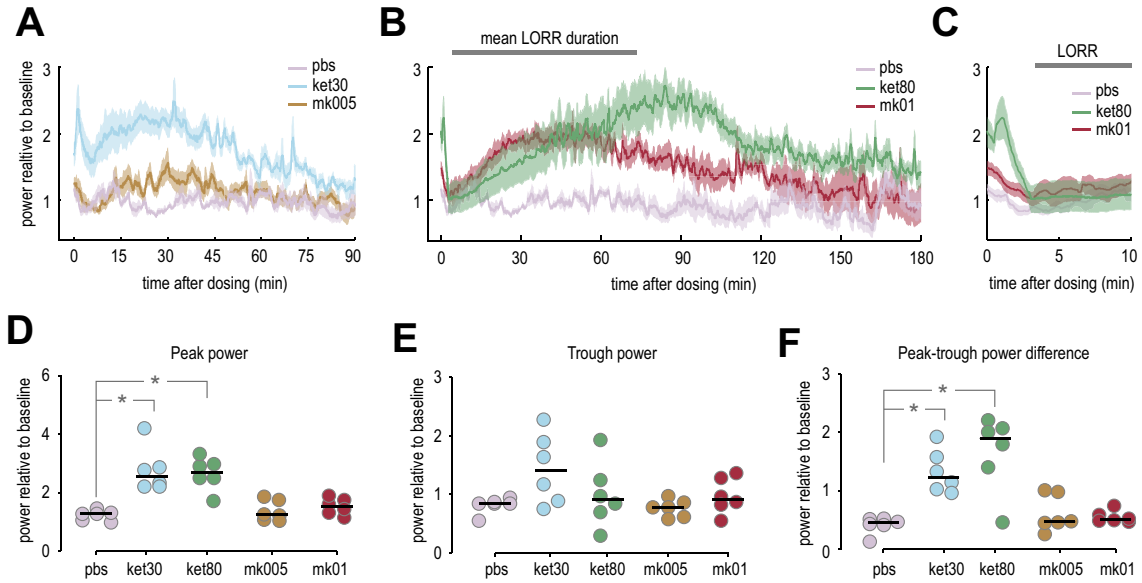

Figure 4. The time course of HFO power after ketamine injection shows a triphasic curve. (A) Time course of power in the 130–160 Hz band (mean ± SEM) after dosing of PBS (lavender), 0.05 mg/kg of MK-801 (brown), and 30 mg/kg of ketamine (light blue). All curves were standardized relative to baseline. (B) Time course of power in the 130–160 Hz band after injections of PBS (lavender), 0.1 mg/kg of MK-801 (red), and 80 mg/kg of ketamine (green). The grey horizontal line corresponds to the mean duration of LORR after the injection of 80 mg/kg of ketamine. (C) Enlargement of the first ten minutes of the curves shown in (B), showing the initial peak in HFO power observed after ketamine dosing. (D) Peak power of the HFO is significantly different than PBS after only after ketamine dosing (Kruskal-Wallis ANOVA $p \ll 0.001$). (E) The power at the trough of the HFO power is not different from PBS (Kruskal-Wallis ANOVA $p = 0.19$). (F) The difference between peak and trough HFO power is significantly different from PBS only after ketamine dosing (Kruskal-Wallis ANOVA $p = 0.002$). Color code in D–F same as in A and B.

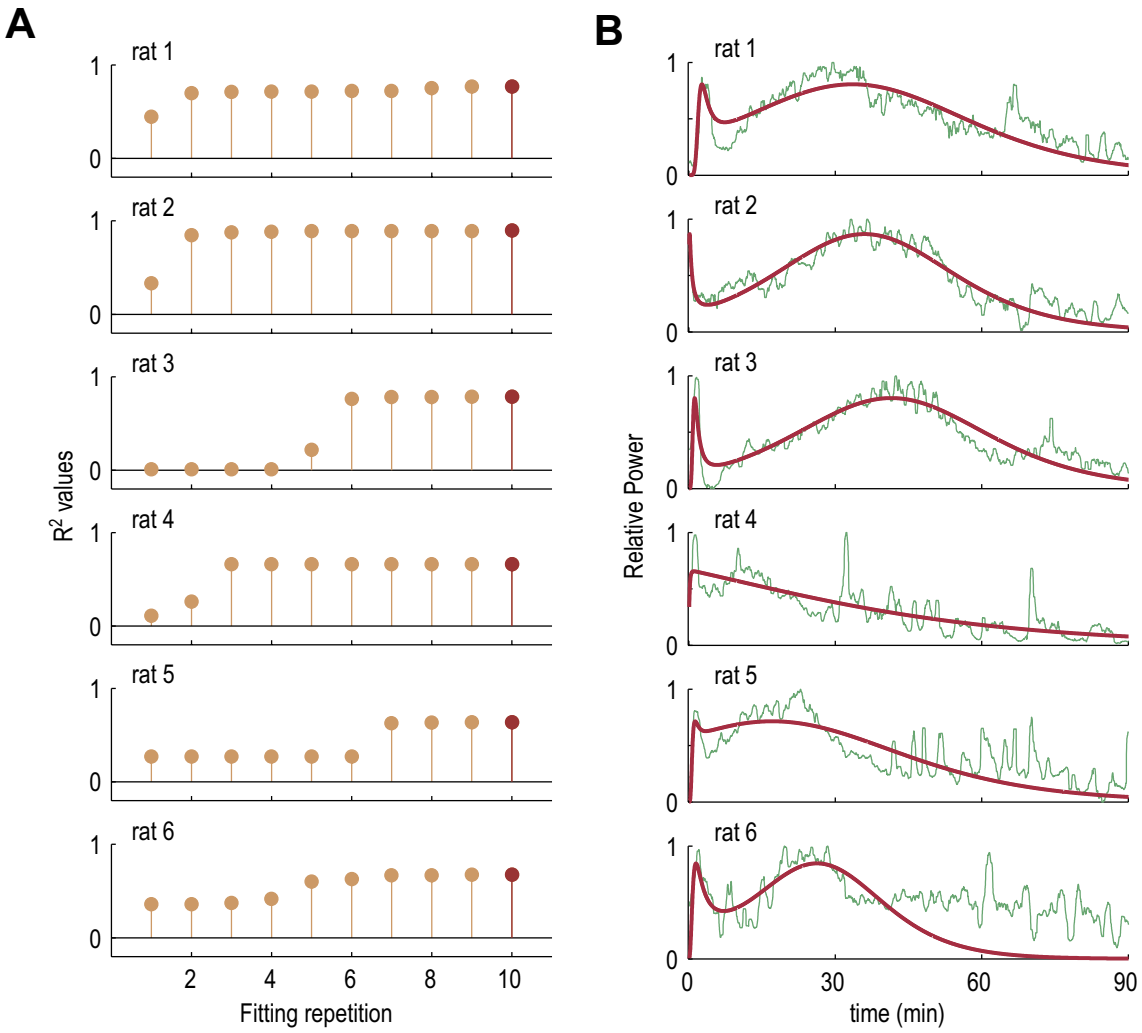

Figure 5. Coefficient of determination (R^2) and model fits for the low dose of ketamine. (A) Sorted R^2 values obtained from each of the 10 repetitions of the fitting procedure, in each of the 6 rats, after dosing of 30 mg/kg of ketamine. The maximum R^2 is shown in dark grey at the end of the series. (B) The plots show the time course of each individual HFO power (light grey, n = 6), standardized between 0 and 1. Superimposed is the fit $HFO(C_b, t)$ (dark grey) with the maximum R^2 value.

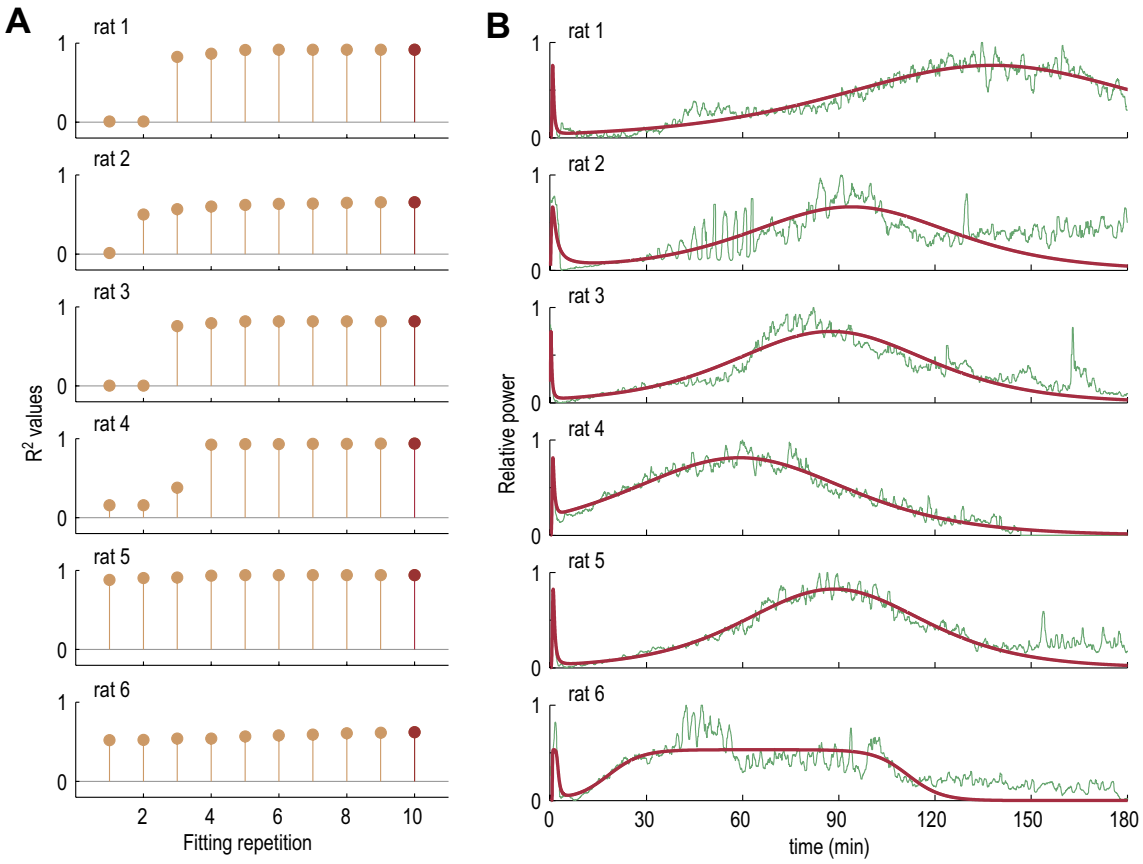

Figure 6. Coefficient of determination (R^2) and model fits for the high dose of ketamine. (A) Sorted R^2 values obtained from each of the 10 repetitions of the fitting procedure, in each of the 6 rats, after dosing of 80 mg/kg of ketamine. The maximum R^2 is shown in dark grey at the end of the series. (B) The plots show the time course of each individual HFO power (light grey, n = 6), standardized between 0 and 1. Superimposed is the fit $HFO(C_b, t)$ (dark grey) with the maximum R^2 value.

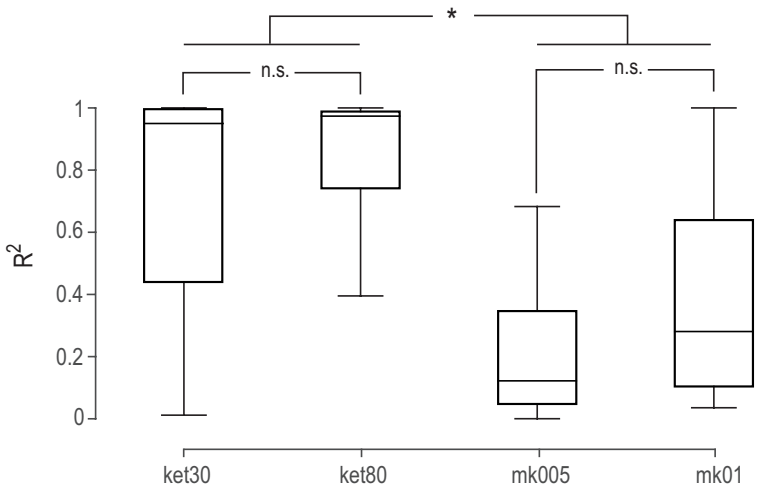

Figure 7. Comparison of R^2 values obtained from fits to HFO instantaneous power induced by ketamine and MK-801. Boxplots of the R^2 values (n = 60) obtained from the 10 repetitions of the fitting procedure in each of the 6 rats after dosing of 30 mg/kg of ketamine, 80 mg/kg of ketamine, 0.05 mg/kg of MK-801, and 0.1 mg/kg of MK-801. The horizontal line in the boxplots is the median, and the box covers the interquartile range. The whiskers are set to cover 99.3% of the data if this were normally distributed. The R^2 values obtained from the fit of 30 and 80 mg/kg of ketamine are significantly higher than those after dosing 0.05 and 0.1 mg/kg of MK-801 ($p \ll 0.001$). The R^2 values are not different between the fits to ketamine ($p = 0.89$) or between the fits to MK-801 ($p = 0.14$).

Tables

Table 1. Parameters of the PK-PD for the best fits after the injection of the lower dose of ketamine (30 mg/kg)

Subject	k_{ab}	k_{ba}	k_{el}	$EC_{50,+}$	$EC_{50,-}$	HFO_{max}	N	R^2
rat 1	0.05166	0.5647	0.007713	0.06513	0.06855	0.8058	8.898	0.77
rat 2	0.2285	0.3831	0.1189	0.02956	0.03554	0.8669	1.197	0.89
rat 3	0.2967	0.3775	0.02706	0.2372	0.2395	0.8024	5.065	0.78
rat 4	0.2836	4.891	0.03203	0.1456	0.1636	0.6561	0.9966	0.66
rat 5	0.2025	1.186	0.01385	0.1198	0.1202	0.7150	4.795	0.63
rat 6	0.02269	0.2911	0.04921	0.02079	0.03121	0.8463	2.555	0.67

k_{ab}, k_{ba} and k_{el} are in min^{-1}. $EC_{50,+}$, $EC_{50,-}$, HFO_{max}, N and R^2 are adimensional.

Table 2. Parameters of the PK-PD model for the best fits after the injection of the higher dose of ketamine (80 mg/kg)

Subject	k_{ab}	k_{ba}	k_{el}	$EC_{50,+}$	$EC_{50,-}$	HFO_{max}	N	R^2
rat 1	0.2460	0.4332	0.01403	0.09624	0.1173	0.7376	3.367	0.91
rat 2	0.3117	0.5756	0.007089	0.2236	0.2358	0.7224	11.04	0.65
rat 3	0.4804	1.045	0.01916	0.09759	0.1038	0.7491	3.768	0.81
rat 4	0.2851	1.2345	0.007344	0.1323	0.1323	0.8153	7.485	0.93
rat 5	1.6509	0.3672	0.05443	0.3221	0.3614	0.8221	5.467	0.94
rat 6	0.007622	0.9248	0.01713	0.001241	0.006267	0.5355	8.5790	0.61

k_{ab}, k_{ba} and k_{el} are in min^{-1}. $EC_{50,+}$, $EC_{50,-}$, HFO_{max}, N and R^2 are adimensional.